Fuzzy Logic and Singular Value Decomposition based Through Wall Image Enhancement

Muhammad Mohsin RIAZ, Abdul GHAFOOR

Department of Electrical Engineering, Military College of Signals, National University of Sciences and Technology (NUST), Islamabad, Pakistan

mohsinriaz@mcs.edu.pk and abdulghafoor-mcs@nust.edu.pk

Abstract. *Singular value decomposition based through wall image enhancement is proposed which is capable of discriminating target, noise and clutter signals. The overlapping boundaries of clutter, noise and target signals are separated using fuzzy logic. Fuzzy inference engine is used to assign weights to different spectral components. K-means clustering is used for suitable selection of fuzzy parameters. Proposed scheme significantly works well for extracting multiple targets in heavy cluttered through wall images. Experimental results are compared on the basis of mean square error, peak signal to noise ratio and visual inspection.*

Keywords

Through wall imaging, Image enhancement, Singular value decomposition, Fuzzy logic, K-means clustering.

1. Introduction

Through Wall Imaging (TWI) is an active research area due to its wide range of applications (especially in rescue, military, surveillance and remote sensing). TWI (seeing through opaque materials) gives the ability to examine building structure layout, detection and localization of target(s). Compared to other remote sensing techniques (ground penetrating radar and medical imaging), TWI has to deal with variety of challenges (propagation environment, sensor positioning and operational requirements). Moreover, propagation medium (often composed of multiple unknown, non-homogenous and non-uniform walls) leads to multi-paths and strong clutters which makes TWI a complex and challenging problem [1].

TWI system works on RADAR principle. Electromagnetic pulse of certain frequency is transmitted that reflects from target and is received with some attenuation [2]. Low frequencies provide good penetration through walls but result in poor resolution compared to high frequencies. However, antennas become large at low frequencies which restrict lower frequency range to 1 GHz practically. On the other hand, if we address detection through concrete walls, the upper frequency range is limited to 3 GHz [3].

Hardware setup (antennas, Vector Network Analyzer (VNA) and position controller) and software algorithms for TWI are improving day by day [4]. Once the hardware receive the reflected signals, the first task is to reconstruct image by measuring attenuation coefficient and total flight time. Various methods of image reconstruction in TWI include Kirchhoff migration, f-k migration, differential SAR and beamforming etc [4]. Improvements [1]-[8] are suggested to overcome some limitations (like knowledge of wall parameters, incidence and reflective angles, homogenous medium, multiple targets and point target etc). Reconstructed image quality directly affects the target classification accuracy.

Image enhancement in TWI, has enjoyed an increasing interest over last few years. Clutter (mainly due to wall reflections) and noise result in degradation of image quality, ambiguity in localization of targets and appearance of false targets. Techniques for image enhancement in TWI include, background subtraction [9], spatial filtering [10], wall parameter estimation/modeling based [11], [12], doppler domain filtering [13], image fusion [14], [15] and statical methods [16]-[20].

Major drawback of background subtraction technique is that it requires a surveillance mode of operation in which there is an access to the background (image scene that is free from targets) or reference [9]. Spatial filtering relies on invariance of wall characteristic (where wall return remains the same with changing antenna location). Moreover, this scheme works only for homogeneous (or near-homogeneous) walls at low operating frequencies [10]. Limitation of wall parameter estimation/modeling based approach is that it requires accurate modeling and parameter estimation [11]. Doppler domain filtering assumes that background is stationary and targets are moving so a doppler shift occurs which can be used to discriminate target and clutter signals [13]. Image fusion methods require multiple images of same scene from different locations (which is not possible especially in case of moving targets) [14], [15]. Some statistical methods for TWI enhancement include Singular Value Decomposition (SVD), Factor Analysis (FA), Principal Component Analysis (PCA) and Independent Component Analysis (ICA) [16]-[20]. Statistical methods having

less computational complexity and provide comparable results to other image enhancement methods. However these methods (SVD, PCA, FA and ICA) suffer from limitation that total number of targets are required to be known a-priori. Statistical methods sometimes also require a subjective threshold value.

Fuzzy logic and SVD (FSVD) based image enhancement is proposed for TWI which provides better accuracy compared to existing SVD based image enhancement. SVD is chosen for its low complexity and simplicity over other methods (PCA, FA and ICA). Proposed method successfully estimates total number of targets and result in improved image quality. Proposed scheme significantly works well for extracting multiple targets in heavy cluttered TWI image. Existing and proposed algorithms are compared on the basis of Mean Square Error (MSE), Peak Signal to Noise Ratio (PSNR) and visual inspection.

2. Image Enhancement

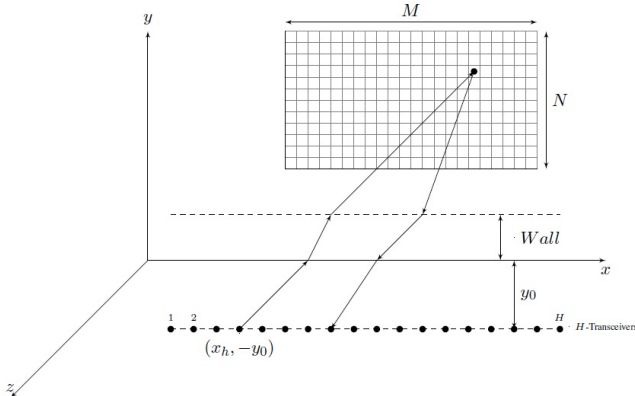Geometrical representation of TWI is shown in Fig. 1.

Fig. 1. Geometrical representation of TWI.

Let H transceivers be placed (parallel to the x-axis) in the $x - y$ plane. Image region (located beyond the wall along the positive y-axis) is divided into grid of $M \times N$ pixels ($m = 1, 2, 3..., M$ and $n = 1, 2, 3..., N$). Let $\theta(t)$ be a wideband transmitted signal then pixel value at location mn can be computed by weighted sum and delay beamforming [4]. Output $\zeta_{mn}(t)$ for target located in $x - y$ plane at pixel location mn is given by:

$$\zeta_{mn}(t) = \sum_{p,q}^{H} \xi(p,q) \vartheta(t + \hat{\tau}_{mn}(p,q)) \qquad (1)$$

where $\xi(p,q)$ are weights (normally based on Kaiser or Hamming window) used to control side lobes and $\hat{\tau}_{mn}(p,q)$ are applied focusing delays and can be calculated by various methods depending on the available wall information [4]. Received signal $\vartheta(t)$ is a delayed version of transmitted signal $\theta(t)$ with some attenuation $\alpha_{mn}(p,q)$ i.e. $\vartheta_{mn}(t) = \alpha_{mn}(p,q)\theta(t - \tau_{mn}(p,q))$ where $\tau_{mn}(p,q)$ are time delays. Let $\hat{\theta}(t) = \theta(-t)$ be a filter matched to transmitted signal

then the de-convoluted output for pixel mn, f_{mn} is given as:

$$f_{mn} = (\zeta_{mn}(t) * \hat{\theta}(t))\big|_{t=0} \qquad (2)$$

$$= \left(\sum_{p,q}^{H} \alpha_{mn}(p,q)\xi(p,q)\theta(t - \tau_{mn}(p,q) + \hat{\tau}_{mn}(p,q)) * \hat{\theta}(t) \right)\Bigg|_{t=0}$$

The above process is repeated for each pixel location mn to obtain B-scan image

$$F = \begin{pmatrix} f_{11} & f_{12} & \cdots & f_{1N} \\ f_{22} & f_{22} & \cdots & f_{2N} \\ \vdots & \vdots & \ddots & \vdots \\ f_{M1} & f_{M2} & \cdots & f_{MN} \end{pmatrix}. \qquad (3)$$

2.1 SVD Based Image Enhancement

Image enhancement in TWI can be performed by decomposing B-scan X into different spectral components using singular value decomposition, i.e.

$$F = USV^T$$
$$= s_1 \begin{bmatrix} \vdots \\ u_1 \\ \vdots \end{bmatrix} [\dots v_1^T \dots] + \cdots + s_M \begin{bmatrix} \vdots \\ u_M \\ \vdots \end{bmatrix} [\dots v_M^T \dots] \quad (4)$$

where (for simplicity $M \le N$), $U = \begin{bmatrix} u_1 & u_2 & \cdots & u_M \end{bmatrix}$ and $V = \begin{bmatrix} v_1 & v_2 & \cdots & v_N \end{bmatrix}$ having dimensions $M \times M$ and $N \times N$ are called unitary matrices and computed as left FF^T and right $F^T F$ eigen vectors respectively. Let $S = diag(s_1, s_2, ..., s_M)$ with $s_1 \ge s_2 \ge ... \ge s_M \ge 0$, are singular values of F;

$$F = \sum_{m=1}^{M} s_m u_m v_m^T = \sum_{m=1}^{M} F_m \qquad (5)$$

where F_m are matrices of same dimensions as F and are called modes (or m^{th} singular image) of F. Image F can be decomposed into three subspaces as:

$$F = \sum_{m=1}^{k_1} s_m u_m v_m^T + \sum_{m=k_1+1}^{k_2} s_m u_m v_m^T + \sum_{m=k_2+1}^{M} s_m u_m v_m^T \quad (6)$$

where the first k_1 singular values belong to wall clutters followed by k_2 singular values belonging to target(s) and the remaining singular values represent noise. *Verma et al.* in [17], [18] state that $k_1 = 1$ for wall clutter and $k_2 = 2$ for target subspaces and rest subspaces represents noise, i.e. the target image F_{SVD} is

$$F_{SVD} = s_2 u_2 v_2^T. \qquad (7)$$

However, we note that this statement ($k_2 = 2$) is not true in case of multiple targets. In fact, the target subspace can be more than one dimensional even when only a single target is present in the scene. Therefore, some statistical analysis needs to be performed in order to determine value for k_2. In this regard some schemes in literature include difference

of singular values ($\Delta s_m = s_m - s_{m+1}$), ratio of singular values (s_m/s_{m+1}) and percent of total power in a singular value ($s_m/tr[F]$) [21]. However, these schemes do not always provide satisfactory results (and sometimes require an empirical threshold setting).

2.2 Fuzzy SVD Based Image Enhancement

It is observed that the boundaries of clutter, noise and target signals are not sharply defined. Therefore, it is not possible to extract target singular values accurately. This motivates use of weights to sharpen the boundaries of clutter, noise and target signals. It is observed that when s_m and Δs_m are high, then s_m possibly belongs to target and need to be enhanced by applying heavy weights. Otherwise s_m belongs to noise and clutter and needs to be suppressed by assigning light weights. Fig. 2 describes this concept.
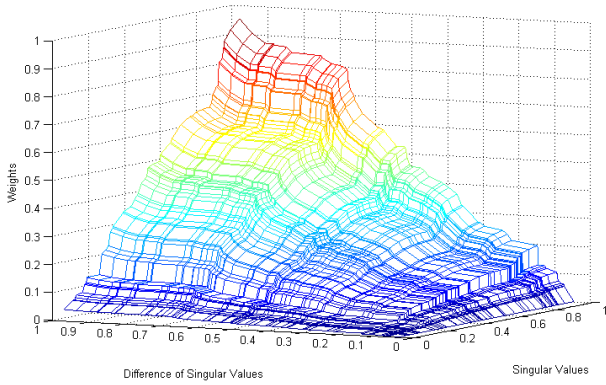

Fig. 2. Illustration of weight assignment criteria.

Let w_m be the weight assigned to m^{th} singular value, then the target image using fuzzy SVD is F_{FSVD}:

$$F_{FSVD} = \sum_{m=2}^{M} F_m w_m = \sum_{m=2}^{M} w_m s_m u_m v_m^T. \tag{8}$$

Various weight assignment techniques (like linearly weights, exponentially weights, logistic weights, fuzzy weights etc) are available in literature but are never explored (to the best of authors's knowledge) for TWI image enhancement. Some weighting schemes are defined as:

- Linear weights

$$w_m = \frac{\psi_1 s_m + \psi_2 \Delta s_m}{\psi_3}, \tag{9}$$

- Exponential weights

$$w_m = \frac{e^{(\psi_1 s_m + \psi_2 \Delta s_m)}}{\psi_3}, \tag{10}$$

- Logistic weights

$$w_m = \frac{\psi_3}{1 + e^{-(\psi_1 s_m + \psi_2 \Delta s_m)}} \tag{11}$$

where ψ_1 and ψ_2 are constants used to control the effect of s_m and Δs_m respectively and ψ_3 is normalizing constant. The above weight assignment techniques appear simple to use but their main drawback is empirical determination of constants (ψ_1, ψ_2 and ψ_3). Note that, weight assignment using fuzzy logic is automatic therefore we use it for TWI image enhancement. Fig. 3 shows block diagram of a fuzzy system.
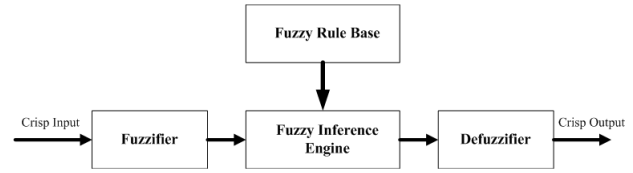

Fig. 3. Fuzzy system.

2.2.1 Gaussian Fuzzifier (GF)

Let singular values s_m and difference of singular values Δs_m may be represented in vector notation as:

$$\mathbf{x}^* = [x_1^* \quad x_2^*] = [s_m \quad \Delta s_m] \tag{12}$$

where $\mathbf{x}^* \in R^2$ represents real value points. We define gaussian Membership Functions (MF) $\mu_{A^d}(x_1)$ and $\mu_{B^e}(x_2)$ for inputs as:

$$\mu_{A^d}(x_1) = e^{-\left(\frac{x_1 - \bar{x}_1^{(d)}}{\sigma_1^{(d)}}\right)^2}, \tag{13}$$

$$\mu_{B^e}(x_2) = e^{-\left(\frac{x_2 - \bar{x}_2^{(e)}}{\sigma_2^{(e)}}\right)^2} \tag{14}$$

where $d = 1, 2, 3$ and $e = 1, 2, 3$ represents the number of fuzzy sets. $\bar{x}_1^{(d)}$, $\bar{x}_2^{(e)}$ and $\sigma_1^{(d)}$, $\sigma_2^{(e)}$ are constant parameters representing means and variances of fuzzy sets. GF is used to map $\mathbf{x}^* \in R^2$ into fuzzy set AB having following gaussian MF:

$$\mu_{AB}(x_1, x_2) = e^{-\left(\frac{x_1 - x_1^*}{a_1}\right)^2} \star e^{-\left(\frac{x_2 - x_2^*}{a_2}\right)^2} \tag{15}$$

where $\star$ is t-norm operator and is taken as algebraic product. a_1 and a_2 are positive parameters used for noise suppression in input data (e.g. if a_1 and a_2 are larger than $\sigma_1^{(d)}$, $\sigma_2^{(e)}$ the noise will be greatly suppressed so one can choose $a_1 = 2 \max_{d=1}^{3} \sigma_1^{(d)}$ and $a_2 = 2 \max_{e=1}^{3} \sigma_2^{(e)}$. GF has the advantage over other fuzzifiers in terms of accuracy [23], [22].

2.2.2 Product Inference Engine (PIE)

PIE process fuzzy inputs based on fuzzy rule base and linguistic rules. PIE structure consists of individual rule based inference with union combination, Mamdani product implication, algebraic product for t-norm and max operator

for s-norm [22]. Fuzzy IF-THEN rules for noise and clutter reduction are defined on experimental observations that the singular values of target signals have high magnitude and spread compared to noise signals. Fuzzy rule-base decision matrix for image enhancement is shown in Fig. 4.
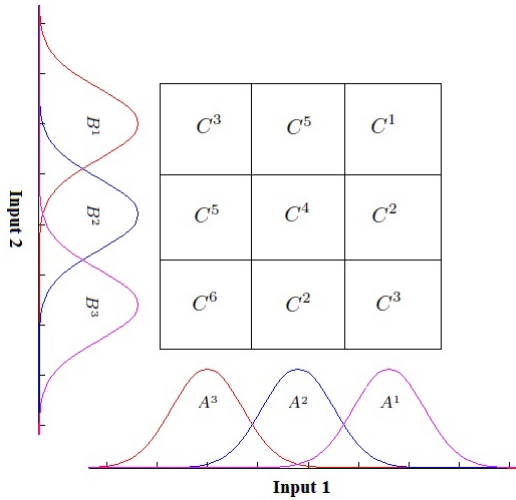

Fig. 4. Decision matrix.

$Ru^{(1)}$: IF s_m is A^1 and Δs_m is B^1 THEN y_m is C^1.

$Ru^{(2)}$: IF s_m is A^1 and Δs_m is B^2 THEN y_m is C^2.

$Ru^{(3)}$: IF s_m is A^1 and Δs_m is B^3 THEN y_m is C^3.

$Ru^{(4)}$: IF s_m is A^2 and Δs_m is B^1 THEN y_m is C^2.

$Ru^{(5)}$: IF s_m is A^2 and Δs_m is B^2 THEN y_m is C^4.

$Ru^{(6)}$: IF s_m is A^2 and Δs_m is B^3 THEN y_m is C^5.

$Ru^{(7)}$: IF s_m is A^3 and Δs_m is B^1 THEN y_m is C^2.

$Ru^{(8)}$: IF s_m is A^3 and Δs_m is B^2 THEN y_m is C^5.

$Ru^{(9)}$: IF s_m is A^3 and Δs_m is B^3 THEN y_m is C^6

where, C^c for $c = 1, 2, .., 6$ are output MFs. A^1, A^2, A^3 and B^1, B^2, B^3 are input fuzzy MFs corresponds to high, medium and low. Similarly C^c are output MFs with C^1 corresponding to highest and C^6 corresponding to lowest.

$$\mu_{C^c}(y_m) = e^{-\left(\frac{y_m - \bar{y}^{(c)}}{\rho^{(c)}}\right)^2} \qquad (16)$$

where $\bar{y}^{(c)}$ and $\rho^{(c)}$ are constant parameters representing mean and variances of output fuzzy sets. PIE is defined as:

$$\mu_{C'}(y_m) = \max_{\{c,d,e\}}\left[\sup_{\{x_1,x_2\}} \mu_{AB}(x_1,x_2)\mu_{A^d}(x_1)\mu_{B^e}(x_2)\mu_{C^c}(y_m)\right]. \qquad (17)$$

Substituting $\mu_{AB}(x_1,x_2)$, $\mu_{A^d}(x_1)$, $\mu_{B^e}(x_2)$, $\mu_{C^c}(y_m)$, the above equation reduces to:

$$\mu_{C'}(y_m) = \max_{\{c,d,e\}}\left[\exp\left[-\left(\frac{x_1 - \bar{x}_1^{(d)}}{\sigma_1^{(d)}}\right)^2 - \left(\frac{x_2 - \bar{x}_2^{(e)}}{\sigma_2^{(e)}}\right)^2 \right.\right.$$
$$\left.\left. - \left(\frac{x_{1T}^d - \bar{x}_1^d}{a_1}\right)^2 - \left(\frac{x_{2T}^e - \bar{x}_2^e}{a_2}\right)^2\right]\mu_{C^c}(y_m)\right] \qquad (18)$$

where

$$x_{1T}^d = \frac{a_1^2\bar{x}_1^d + (\sigma_1^d)^2 x_1^*}{a_1^2 + (\sigma_1^d)^2} \quad \text{and} \quad x_{2T}^e = \frac{a_2^2\bar{x}_2^e + (\sigma_2^e)^2 x_2^*}{a_2^2 + (\sigma_2^e)^2}.$$

2.2.3 Center Average Defuzzifier (CAD)

Fuzzy outputs are converted to real world outputs using defuzzification process. CAD specifies the real output y_m^* as the weighted sum of 6 output fuzzy sets having centers $\bar{y}^{(c)}$ and height $\varpi_m^{(c)}$.

$$w_m = y_m^* = \frac{\sum\limits_{c=1}^{6} \bar{y}^{(c)}\varpi_m^{(c)}}{\sum\limits_{c=1}^{6} \varpi_m^{(c)}}. \qquad (19)$$

CAD has less computational complexity, more accuracy and continuity compared to other defuzzifiers (center of gravity, maximum defuzzifier etc) [22].

2.2.4 Fuzzy Parameters Selection

For designing a fuzzy system, fuzzy parameters selection ($\bar{x}_1^{(d)}$, $\sigma_1^{(d)}$, $\bar{x}_2^{(e)}$, $\sigma_2^{(e)}$ and $\bar{y}^{(c)}$, $\rho^{(c)}$) is important. For fuzzy sets $x_1 \in [0,1]$, $x_2 \in [0,1]$ and $y \in [0,1]$ one way is to assign uniformly distributed Gaussian MFs between zero and one as shown in Fig. 5. However, to further enhance the accuracy, K-means based Fuzzy SVD (KFSVD) is proposed for extracting target image F_{KFSVD} more accurately.

K-means [24] is unsupervised data clustering algorithm that classifies data into a certain number (fixed a priori) of clusters. K-means has applications in various other fields ranging from market segmentation, computer vision, geostatistics, astronomy and agriculture. Below k-means clustering process is used to cluster s_m and Δs_m:

- *Step 1:* Initialize k centroids i.e. one for each cluster. These centroids should be initialized in a cunning way because different initialization leads to different result. Better choice is to place them randomly as far as possible from each other.

- *Step 2:* Assign class labels to data points by using some distance metric (usually euclidian distance is used).

- *Step 3:* Calculate mean (average value) of each class and assign means as new centriods. Repeat above step until the change between new and old centriods becomes negligible.
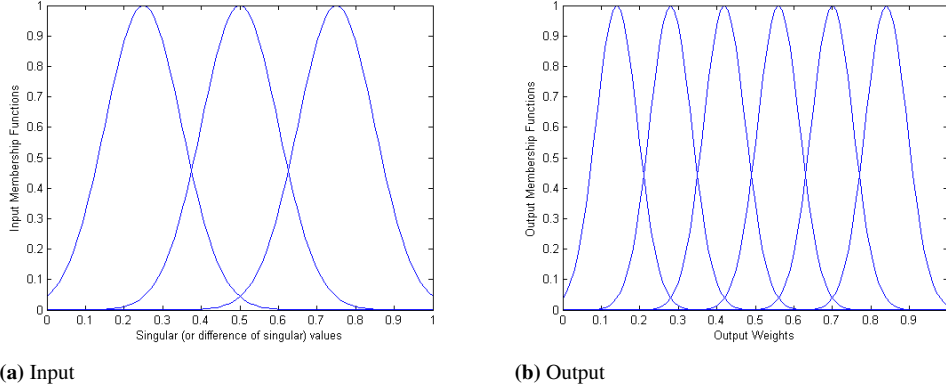
(a) Input   **(b)** Output

Fig. 5. Uniform input and output MFs.

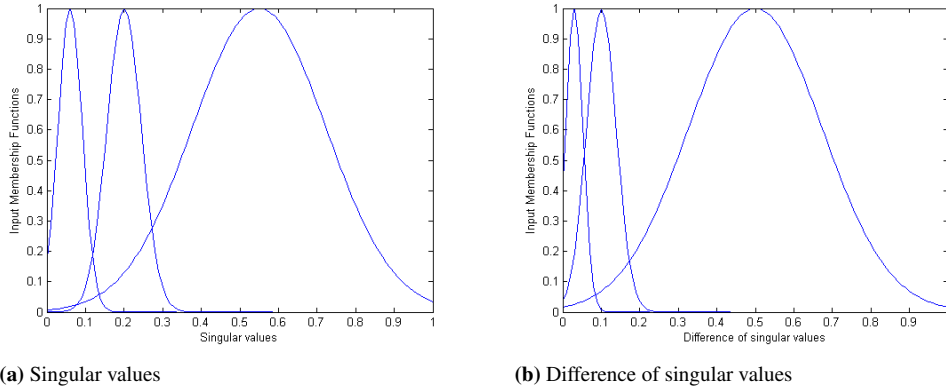**(a)** Singular values   **(b)** Difference of singular values

Fig. 6. Input MFs obtained by k-means.

Once data is clustered the centers $\bar{x}_1^{(d)}$, $\bar{x}_2^{(e)}$ and spread $\sigma_1^{(d)}$, $\sigma_2^{(e)}$ are calculated by mean and variance of that class as shown in Fig. 6 As output distribution is not known a priori, we have used equally spaced output MFs (as discussed earlier). K-means is sensitive to initial randomly selected centers so the algorithm is run multiple times (with different starting points) to get optimized clustering results.

3. Simulation Results

Experimental setup (constructed using [25]) for TWI is shown in Fig. 7 (physical elements of experimental setup are shown in Fig. 8). Agilents's Vector Network Analyzer (VNA) in the range of 300 kHz to 3 GHz is used to generate a stepped frequency 2 GHz to 3 GHz (1 GHz Band Width (BW)) waveform having step size $\Delta f = 5$ MHz and $N_f = 201$. Maximum range R_{max} is calculated as:

$$R_{max} = \frac{c(N_f - 1)}{2BW} = 30 \text{ m.} \qquad (20)$$

The range resolution ΔR is:

$$\Delta R = \frac{c}{2N_f \Delta f} = 0.37 \text{ m.} \qquad (21)$$

Directional and broadband horn antenna with 12 dB gain is used in mono-static mode (for transmitting and receiving signals). Antenna is mounted on 2D-scanning frame (having dimensions: width 2.4 m and height 3 m) which can slide along cross range and height. Rear and side walls are covered with pyramidal radar absorbable modules. Scanning is controlled by micro-controller and at each point scattering parameters (magnitude and phase) are recorded by VNA and transferred to local computer. Wood wall is constructed having thickness 5 cm, relative permittivity (approximately) equals to 2.3 and relative permeability (approximately) equals to 1. The antenna is positioned 0.03 m from the wall. Received data is converted from frequency domain to time domain using inverse fourier transform. Time delays and weights are fed into beamforming algorithm for image reconstruction.

Image enhancement algorithms based on conventional SVD and proposed schemes are simulated in MATLAB. Background subtracted image F_{bs} is constructed using the difference of two images (i.e. image with target and image without target) [25], [9]. This background image is used as a comparison measure for proposed and existing algorithm. Simulation results are compared on the basis of MSE, PSNR and visual inspection.

$$MSE = \frac{1}{M \times N} \sum_{m=1}^{M} \sum_{n=1}^{N} (F_{bs}(m,n) - F_{tar}(m,n))^2, \qquad (22)$$
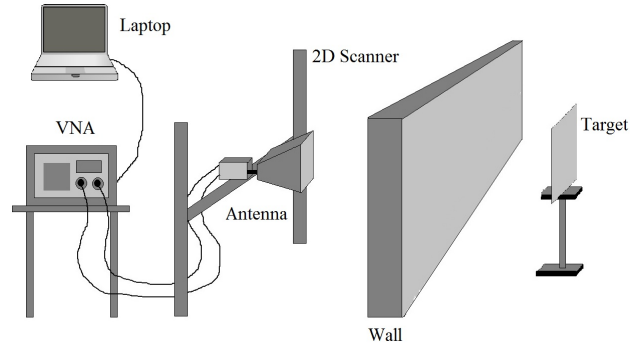
$$PSNR(dB) = 10 \log_{10} \frac{1}{MSE} \qquad (23)$$

Fig. 7. TWI setup.

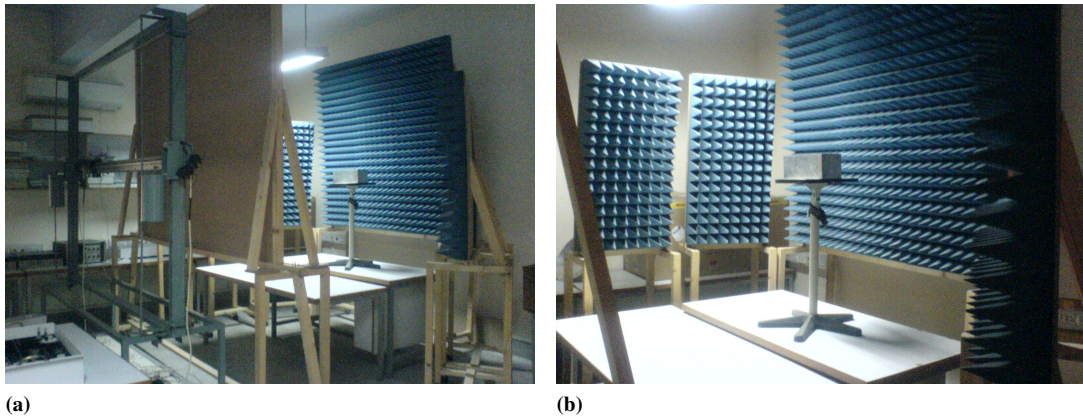
(a)   (b)

Fig. 8. Physical elements of experimental setup at Microwave Engineering Lab, College of Signals, NUST.

where $F_{tar} \in \{F_{SVD}, F_{FSVD}, F_{KFSVD}\}$.

Scenarios	Techniques	MSE	PSNR (dB)
	SVD	0.2814	5.5068
Example 1	FSVD	0.1387	8.5792
	KFSVD	0.1328	8.7680
	SVD	0.3107	5.0766
Example 2	FSVD	0.1521	8.1787
	KFSVD	0.1410	8.5078
	SVD	0.4210	3.7572
Example 3	FSVD	0.1712	7.6650
	KFSVD	0.1682	7.7417

Tab. 1. Comparison of MSE and PSNR(dB) of different schemes.

Images with one, three and five targets were constructed using TWI setup. Fig. 9, Fig. 11 and Fig. 13 show different spectral images (ranging from one to six) for one, three and five targets respectively. Visual inspection shows that the target(s) is/are not limited to second spectral image only, rather some part of target(s) is/are also present in the rest of the spectral images (except the first spectral image). Fig. 10, Fig. 12 and Fig. 14 respectively show one, three and five target(s) singular values, original image, background subtracted image, target and noise image, and images produced using difference image enhancement techniques. It can be seen that proposed schemes significantly work better as compared to conventional SVD scheme and detect all (one, three and five) target(s) accurately whereas conventional SVD scheme fails to accurately detect all target(s).

Results of Fig. 10c, Fig. 12c and Fig. 14c are obtained using conventional SVD scheme defined by (7). Fig. 9b, Fig. 11b and Fig. 13b show the second spectral component of B-scan images. Since the conventional SVD scheme consider that the target is related to second spectral image only so Fig. 10c is same as Fig 9b, Fig. 12c is same as Fig 11b and Fig. 14c is same as Fig 13b.

Note that clutter from wall and additive noise from surroundings are suppressed by use of fuzzy weights. If additional objects have high reflectivity then these objects are inferred as targets (otherwise these objects are inferred as noise) due to comparable singular values with the targets. For example additional object like stool in Fig. 8 has low reflectivity therefore it is part of noise.

Tab. 1 shows the performance comparison of proposed schemes with conventional SVD schemes in terms of MSE and PSNR.

4. Conclusion

Fuzzy logic and SVD based image enhancement technique capable of discriminating between target and clutter signals is proposed for TWI. Proposed schemes are capable
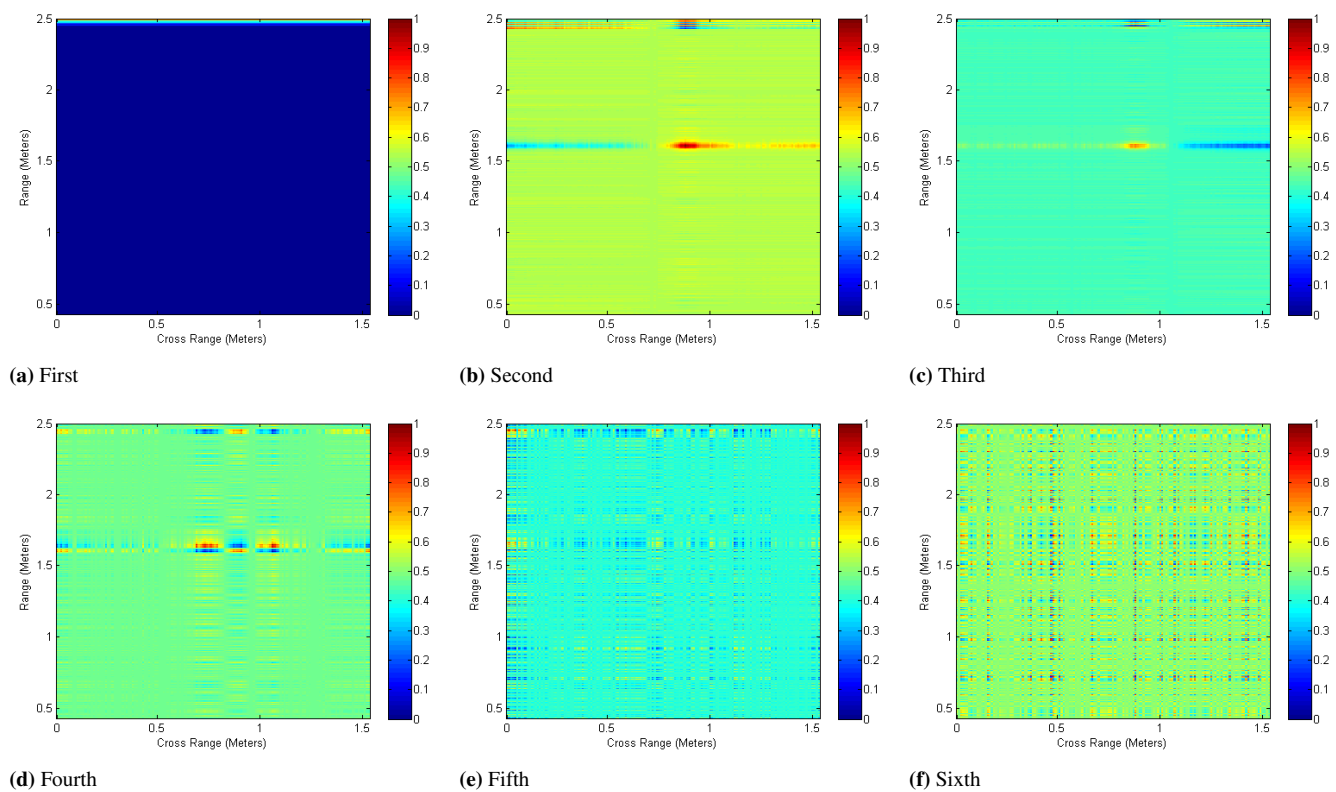
(a) First

(b) Second

(c) Third

(d) Fourth

(e) Fifth

(f) Sixth

Fig. 9. Single target: Different spectral images.

(a)

(b)
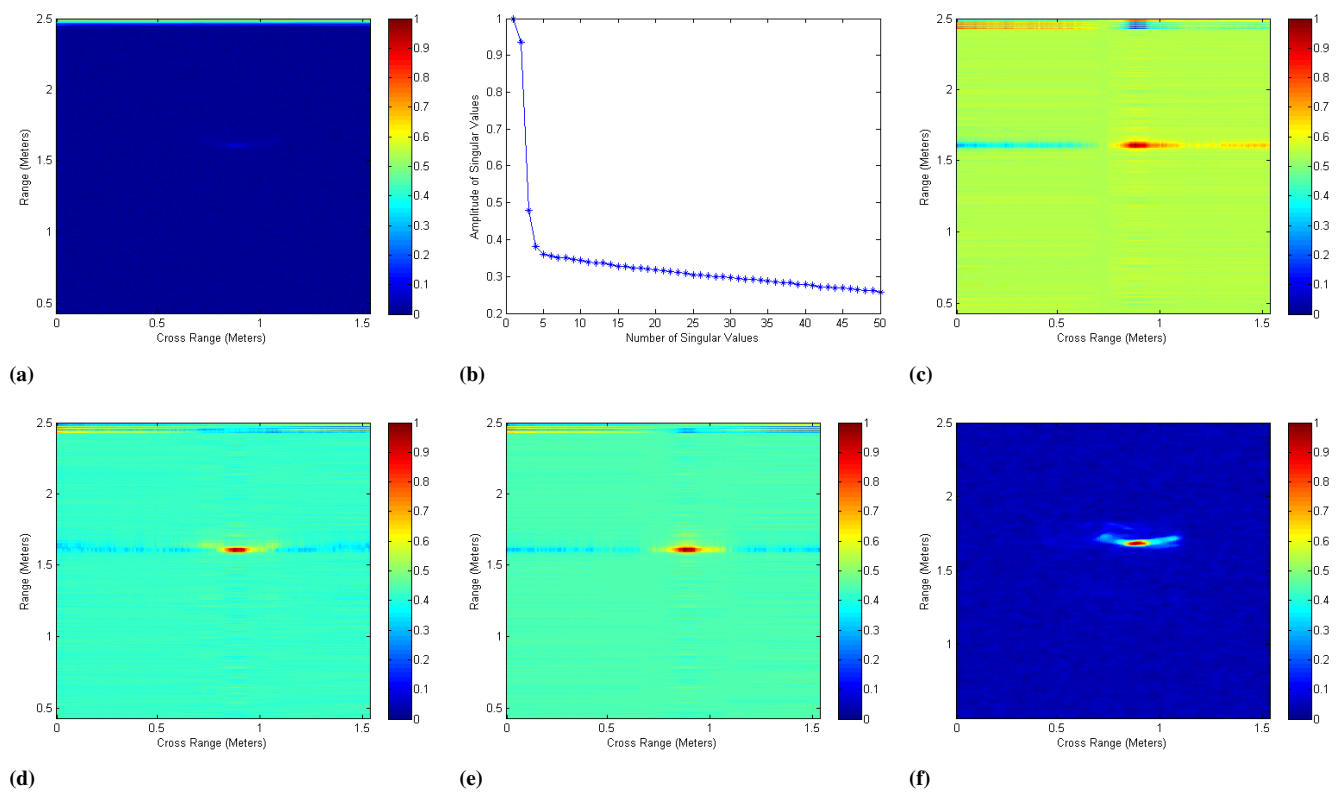
(c)

(d)

(e)

(f)

Fig. 10. Single target; (a) Original image; (b) Singular values; (c) Conventional SVD F_{SVD}; (d) Fuzzy SVD with uniform MF F_{FSVD}; (e) Fuzzy SVD with k-means based MF F_{KFSVD}; (f) Background subtracted image F_{bs}.
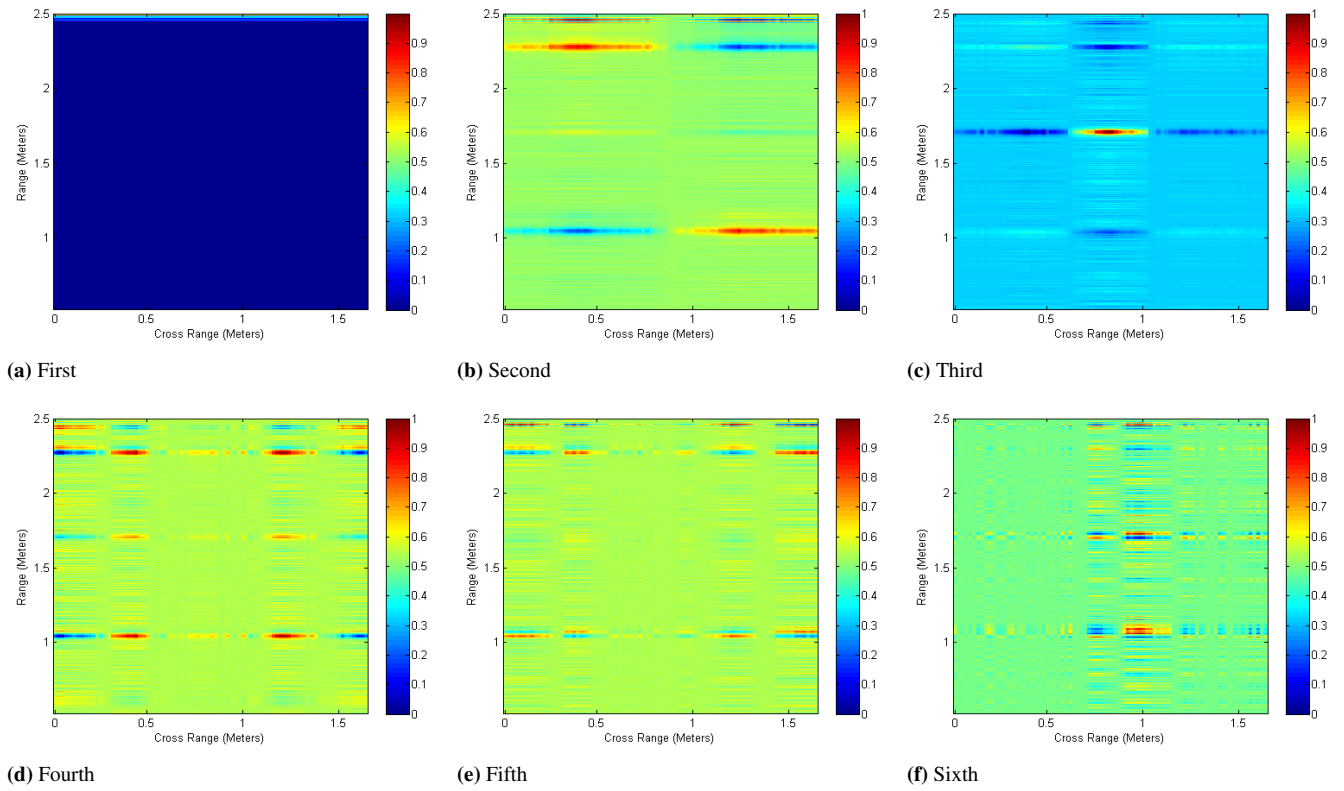
(a) First

(b) Second

(c) Third

(d) Fourth

(e) Fifth

(f) Sixth

Fig. 11. Multiple (three) targets: Different spectral images.

(a)

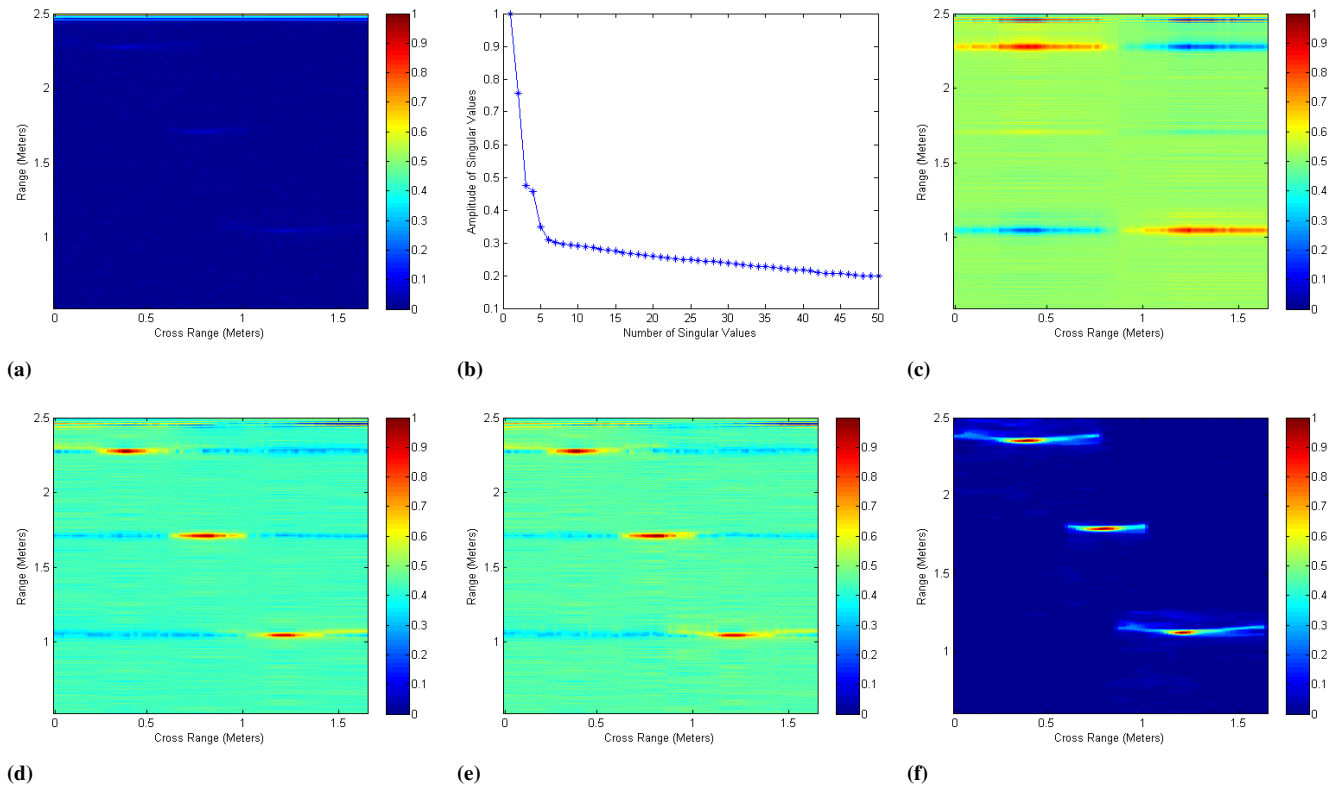**(b)**

(c)

(d)

(e)

(f)

Fig. 12. Multiple (three) targets (a) Original image (b) Singular Values s_m (c) Conventional SVD F_{SVD} (d) Fuzzy SVD with uniform MF F_{FSVD} (e) Fuzzy SVD with k-means based MF F_{KFSVD} (f) Background subtracted image F_{bs}.

(a) First

(b) Second

(c) Third

(d) Fourth

(e) Fifth

(f) Sixth

Fig. 13. Multiple (five) targets: Different spectral images.

(a)

(b)

(c)

(d)

(e)

(f)

Fig. 14. Multiple (five) targets (a) Original image (b) Singular values s_m (c) Conventional SVD F_{SVD} (d) Fuzzy SVD with uniform MF F_{FSVD} (e) Fuzzy SVD with k-means based MF F_{KFSVD} (f) Background subtracted image F_{bs}.
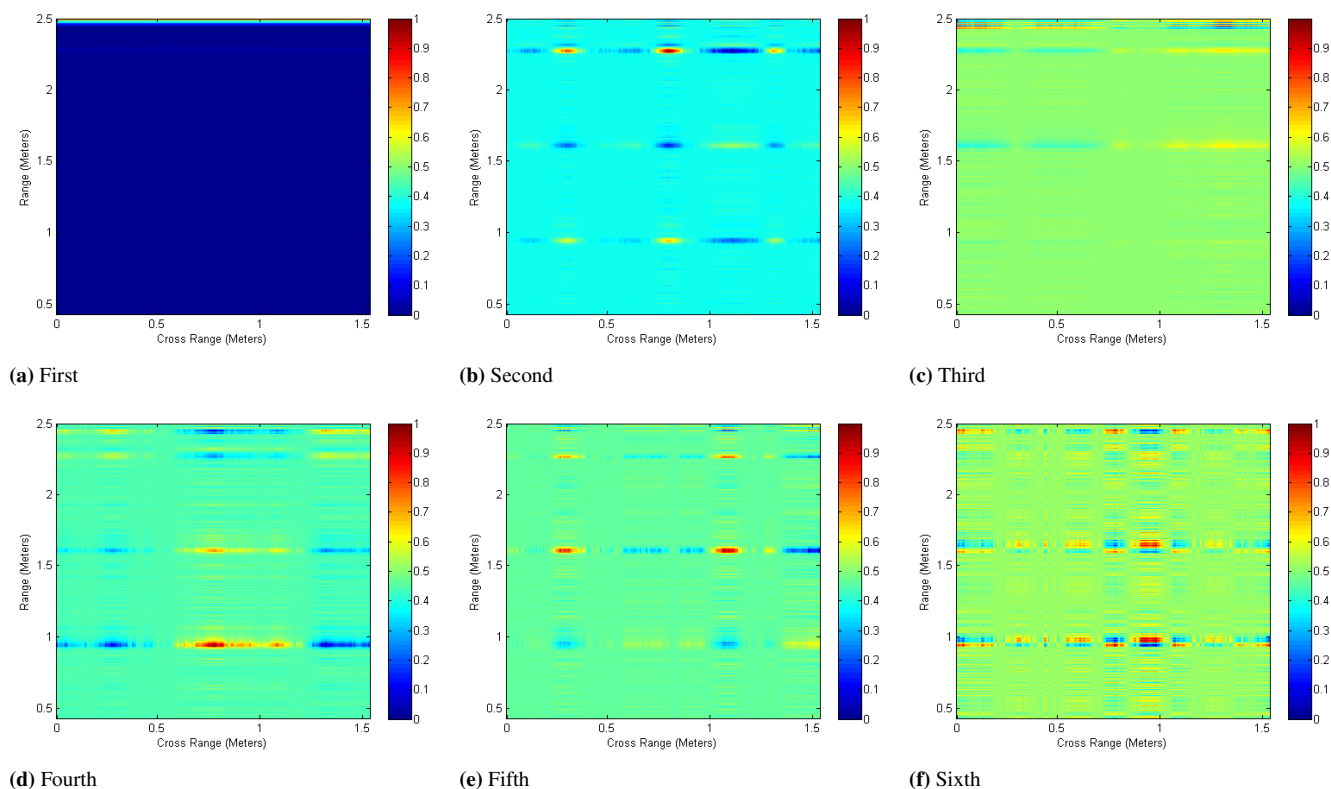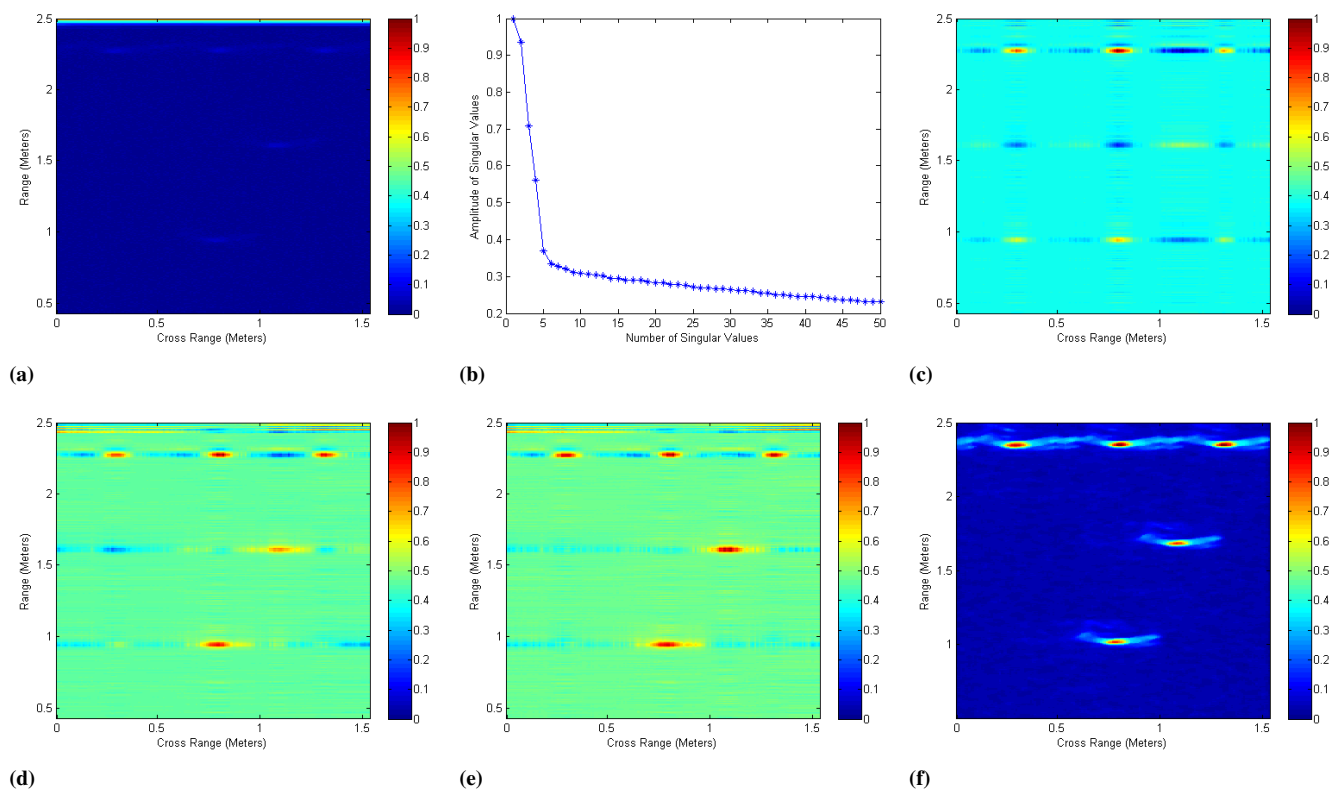
of detecting single and multiple targets in heavy clutter environment. Moreover assigning MF by k-means clustering results in better performance compared to uniform MF. Simulation results show that proposed fuzzy logic based SVD based image enhancement scheme is a significant improvement in conventional SVD based image enhancement. Proposed scheme can also be modified for other statistical methods like PCA, FA and ICA to get better accuracy.

References

[1] BARANOSKI, E. Through-wall imaging: Historical perspective and future directions *Journal of the Franklin Institute*, 2008, vol. 345, no. 6, p. 556 - 569.

[2] FERRIS, D. D., CURRIE, N. C. A survey of current technologies for through the wall surveillance (TWS). *Proceedings of the SPIE*, 1998, vol. 3577, p. 62 - 72.

[3] MUQAIBEL, A., JAZI, A. S., BAYRAM, A., ATTIYA, M., RIAD, S. M. Ultrawideband through-the-wall propagation. *IEE – Proceedings Microwave, Antennas and Propagation*, 2005, vol. 152, pp. 581 - 588.

[4] AMIN, M. G. *Through the Wall Radar Imaging*. Boca Raton (USA): CRC press, 2011.

[5] AFTANAS, M., DRUTAROVSKY, M. Imaging of the building contours with through the wall UWB radar system. *Radioengineering*, 2009, vol. 18, no. 3, p. 258 - 264.

[6] ROVNAKOVA, J., KOCUR, D. Compensation of wall effect for through wall tracking of moving targets. *Radioengineering*, 2009, vol. 18, no. 2, p. 189 - 195.

[7] SCHEJBAL, V., CERMAK, D., NEMEC, Z., PIDANIC, J., KONECNY, J., BEZOUSEK, P., FISER, O. Multipath propagation of UWB through-wall radar and EMC phenomena. *Radioengineering*, 2006, vol. 15, no. 4, p. 52 - 57.

[8] SCHEJBAL, V., BEZOUSEK, P., CERMAK, D., NEMEC, Z., FISER, O., HAJEK, M. UWB propagation through walls. *Radioengineering*, 2006, vol. 15, no. 1, p. 17 - 24.

[9] MOULTON, J., KASSAM, S. A., AHMAD, F., AMIN, M. G., YEMELYANOV, K. Target and change detection in synthetic aperture radar sensing of urban structures. In *Proceedings of IEEE Radar Conference*. Rome (Italy), 2009, p. 1 - 6.

[10] YOON, Y. S., AMIN, M. G. Spatial filtering for wall clutter mitigation in through-the-wall radar imaging. *IEEE Transactions on Geosciences and Remote Sensing*, 2009, vol. 47, no. 9, p. 3192 - 3208.

[11] DEHMOLLAIAN, M., SARABANDI, K. Refocusing through building walls using synthetic aperture radar. *IEEE Transactions on Geosciences and Remote Sensing*, 2008, vol. 46, no. 6, p. 1589 - 1599.

[12] SMITH, G., MOBASSERI, B. G. Robust through-the-wall radar image classification using a target-model alignment Procedure. *IEEE Transactions on Image Processing*, 2012, vol. 21, no. 2, p. 754 - 767.

[13] RAM, S. S., CHRISTIANSON, C., YOUNGWOOK, K., HAO, L. Simulation and analysis of human micro-dopplers in through-wall environments. *IEEE Transactions on Geosciences and Remote Sensing*, 2010, vol. 48, no. 4, p. 2015 - 2023.

[14] DEBES, C. *Advances in Detection and Classification for Through the Wall Radar Imaging*. PhD Dissertation. Darmstadt (Germany): Technische Universität Darmstadt, 2010.

[15] GAIKWAD, A. N., SINGH, D., NIGAM, M. J. Recognition of target in through wall imaging using shape feature extraction. In *IEEE International Geosciences and Remote Sensing Symposium*. Vancouver (Canada), 2011, p. 957 - 960.

[16] CHANDRA, R., GAIKWAD, A. N., SINGH, D., NIGAM, M. J. An approach to remove the clutter and detect the target for ultrawideband through-wall imaging. *Journal of Geophysics and Engineering*, 2008, vol. 5, no. 4.

[17] VERMA, P. K., GAIKWAD, A. N., SINGH, D., NIGAM, M. J. Analysis of clutter reduction techniques for through wall imaging in UWB range. *Progress In Electromagnetics Research B*, 2009, vol. 17, p. 29 - 48.

[18] GAIKWAD, A. N., SINGH, D., NIGAM, M. J. Application of clutter reduction techniques for detection of metallic and low dielectric target behind the brick wall by stepped frequency continuous wave radar in ultra-wideband range. *IET Radar Sonar Navigation*, 2011, vol. 5, no. 4, p. 416 - 425.

[19] GAIKWAD, A. N., SINGH D., NIGAM, M. J. Study of effect of room window on through wall imaging in UWB range. In *International Conference on Emerging Trends in Electronic and Photonic Devices and Systems*. Varanasi (India), 2009, p. 395 - 398.

[20] TIVIVE, F. H., AMIN, M. G., BOUZERDOUM, A. Wall clutter mitigation based on eigen analysis in through the wall radar imaging. *17th Internetional Conference on Digital Signal Processing*. Corfu (Greece), 2011, p. 1-8.

[21] TREES, H. L. V. *Optimum Array Processing*. New York: Wiley, 2003.

[22] WANG, L. X. *A course in fuzzy systems and control*. Upper Saddle River (USA): Prentice Hall, 1997.

[23] YAGER, R., FILEV, D. *Essentials of Fuzzy Modeling and Control*. New York (USA): *Wiley*, USA.

[24] KANUNGO, T., MOUNT, D. M., NETANYAHU, N. S., PIATKO, C. D., SILVERMAN, R., WU, A. Y. An efficient k-means clustering algorithm: analysis and implementation. *IEEE Transactions on Pattern Analysis and Machine Intelligence*, 2002, vol. 24, no. 7, p. 881 - 892.

[25] DILSAVOR, R., AILES, W., RUSH, P., AHMAD, F., KEICHEL, W., TITI, G., AMIN, M. Experiments on wideband through-the-wall imaging. In *Proceedings of SPIE: Algorithm for Synthetic Aperture Radar Imagery XII Conference*. Baltimore (USA), 2005, vol. 5808, p. 196 - 209.